

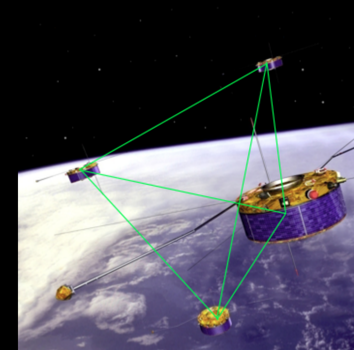

EISCAT Science examples:
Signatures of bursty bulk flows in the ionosphere
and
Ionospheric Joule heating

Anita Aikio, University of Oulu, Finland

Bursty bulk flows (BBFs)

- Transient, localized, fast earthward plasma flows in the central plasma sheet
- Typical duration of 10 min
- V > 400 km/s, cross-tail width 1 – 4 R_E
- Transient magnetic field dipolarization and reduction in plasma density

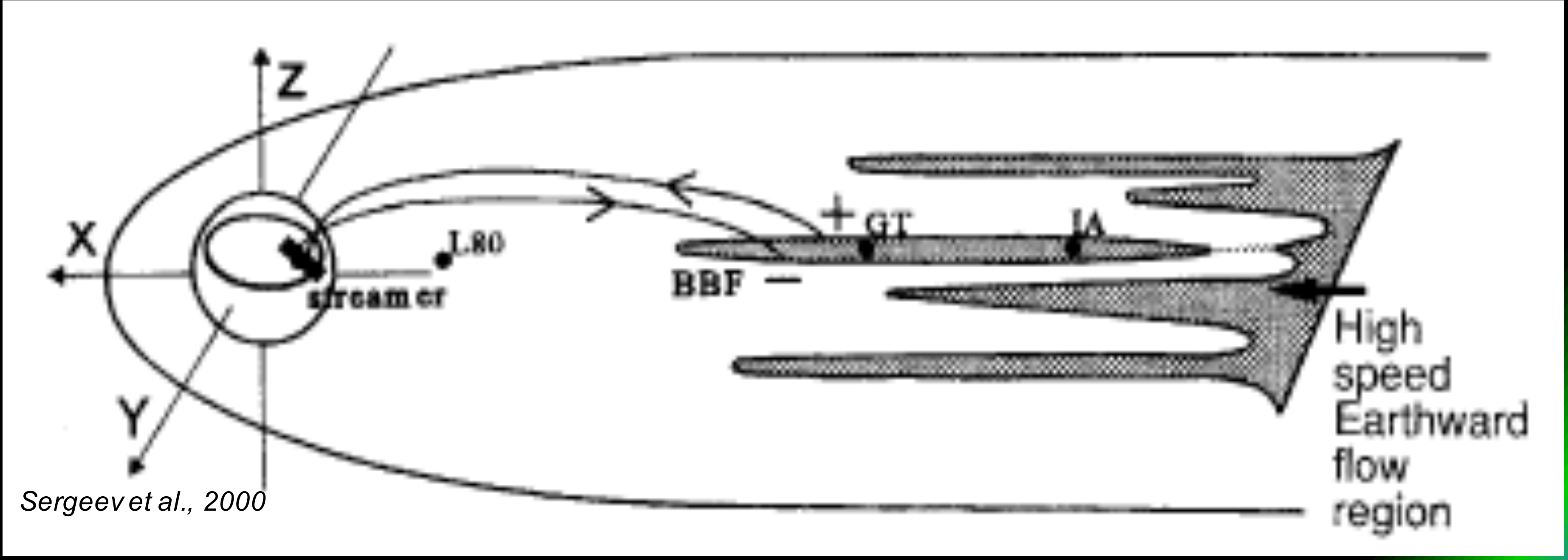

Sergeev et al., 2000

Bursty bulk flow observations

- Cluster satellites were conjugate to EISCAT on 17 Oct 2005. Geomagnetic conditions were quiet.
- Cluster satellites observed several BBFs in the near-Earth plasma sheet (X~-14 Re).
- EISCAT sees signatures of auroral streamers in the ionosphere and specific plasma flow signatures.

Reference: Pitkänen, Aikio, Amm, Kauristie, Nilsson, and Kaila, Ann. Geophys., 2011.

Cluster Observations

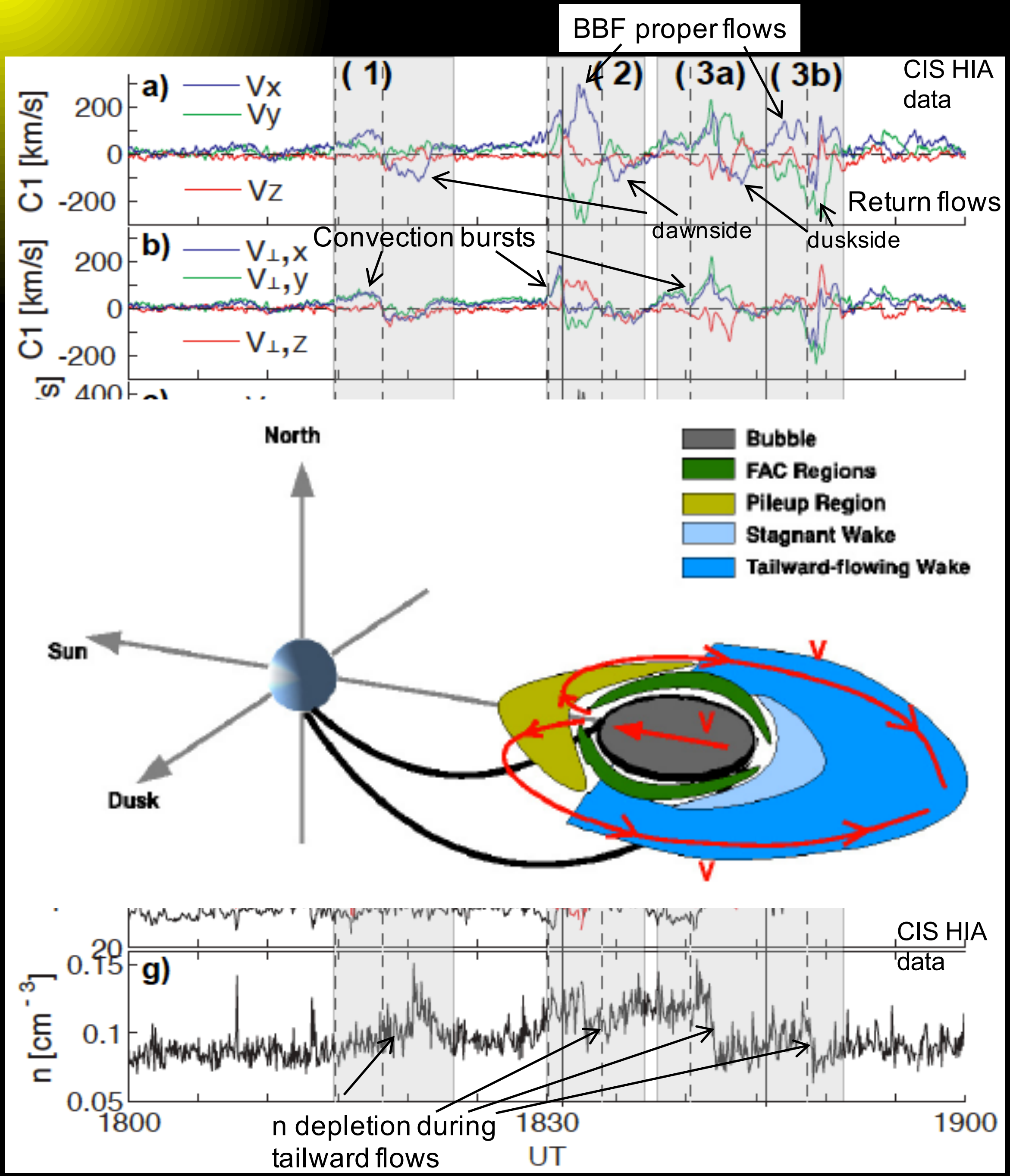

A series of 3 BBF events is identified.

Deflection and compression of ambient plasma in front of an approaching plasma bubble

Tailward flows are consistent with return flow patterns around edges of a bubble and associated with decrease in plasma density which could indicate possible formation of a wake behind the Earthward moving plasma bubble, as suggested by *Walsh et al. (2009)*

EISCAT experiment

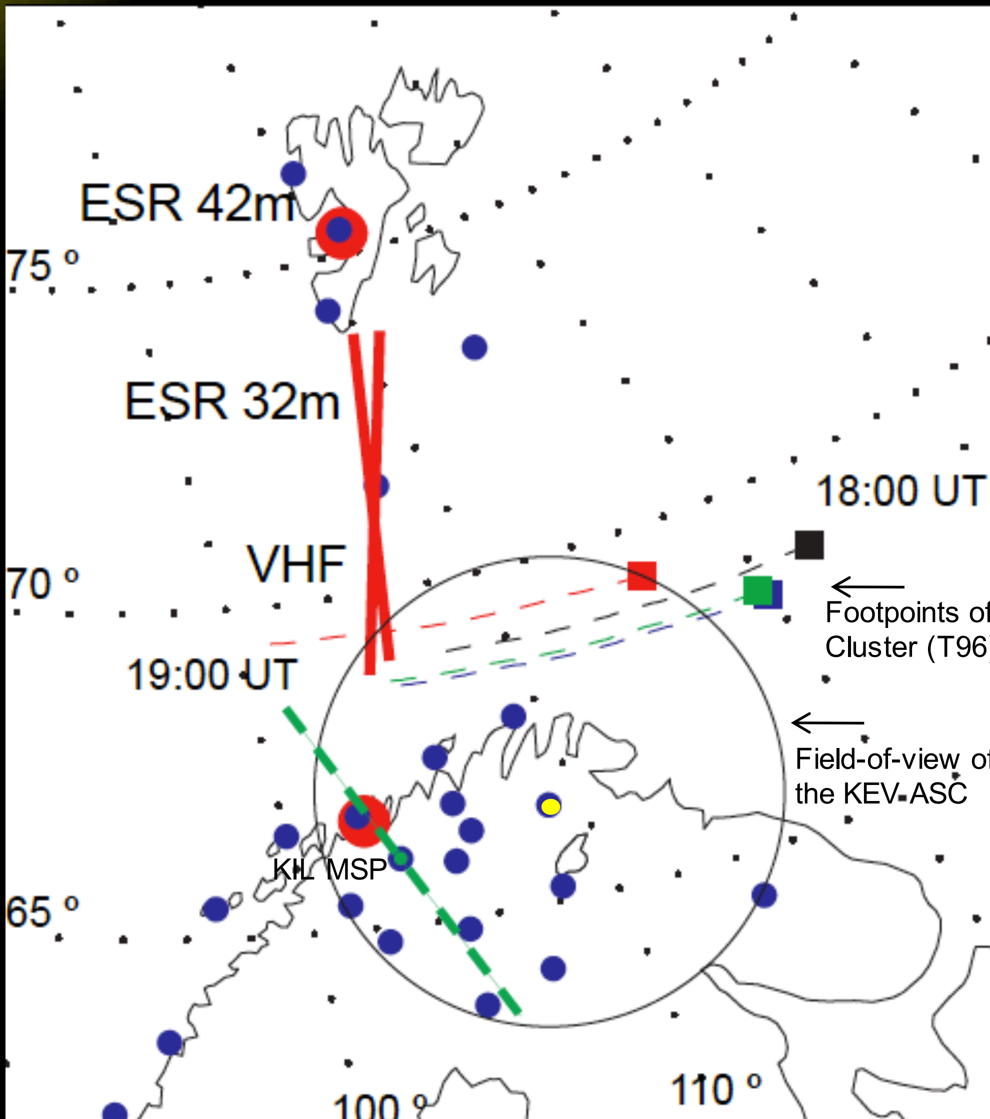

- **VHF pointed at 30º elevation toward North, (ESR32m antenna at 30º to south)**

17 Oct 2005

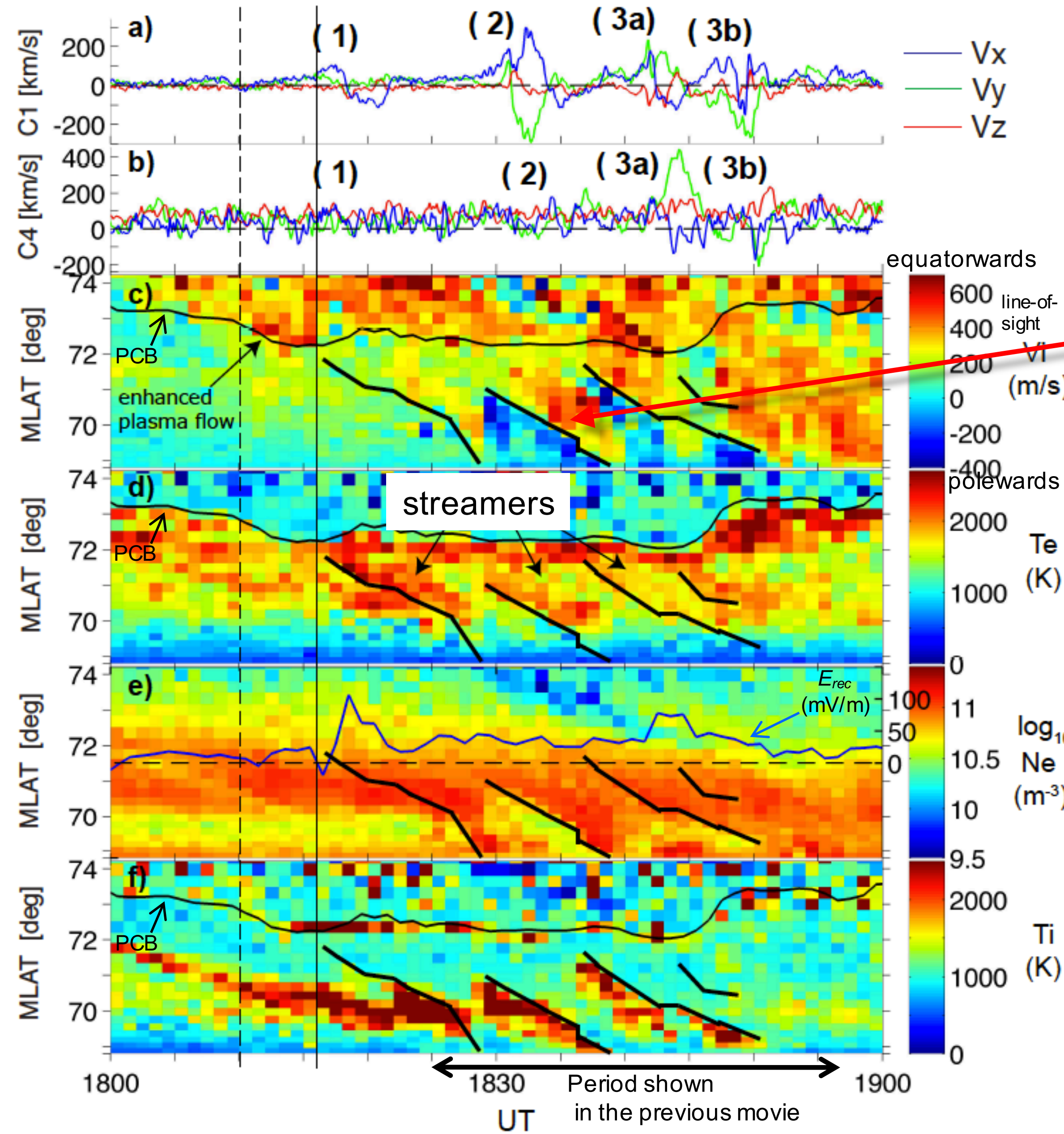

EISCAT VHF

Streamers are associated with

- **Enhancements in Te**
- **Sharp velocity shear at the equatorward edge of a streamer**
- **Equatorward component in the plasma flow within the streamer**
- **Poleward component in the plasma flow on the equatorward side of the streamer ass. with enhanced Ti and reduced Ne**

BBF-streamer (burst 2)

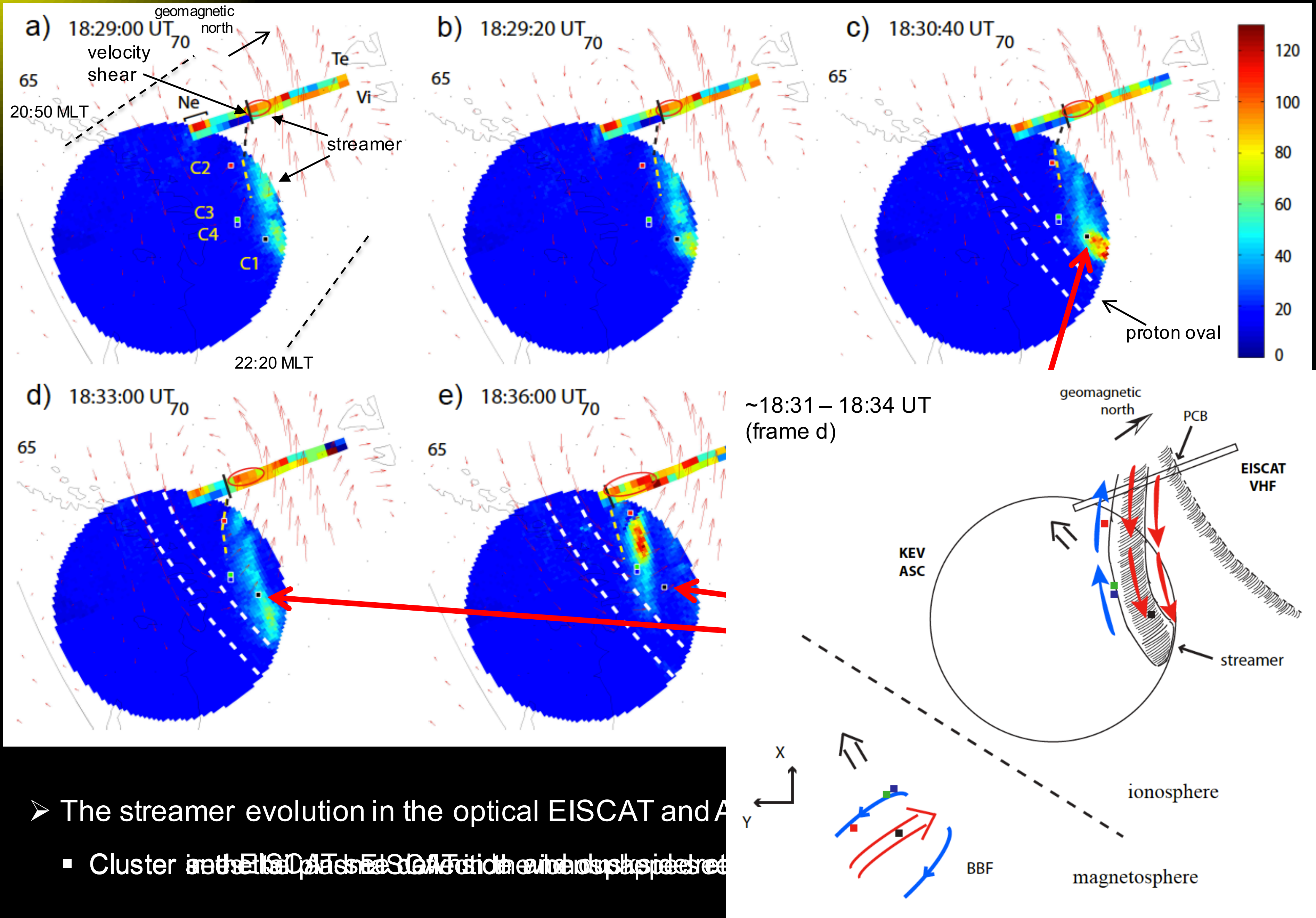

- The streamer evolution in the optical EISCAT and A
  - Cluster

Summary of BBF observations

- Cluster observations suppert the bubble model of the BBFs. The Earthward fast flows measured in the plasma sheet by Cluster satellites are associated with southward plasma flows in the ionosphere measured by the EISCAT radars.
- We showed the first evidence of return flows of a bubble measured simultaneously in the magnetosphere and in the ionosphere.
- Pitkänen et al., AG, 2011

EM energy input into M-I-T system

The solar wind energy penetrating the Earth's magnetosphere goes to:

- Ring current particles (30–60%)
- Plasma sheet heating
- Plasmoids (eventually ejected away from the magnetosphere)
- Particles precipitating into the ionosphere (10–15 %)
- Electromagnetic energy dissipating mainly as Joule heating in the high-latitude ionosphere (30–60 %)
- The estimates above are based on proxies calculated from magnetic indices (AE, Dst, …)

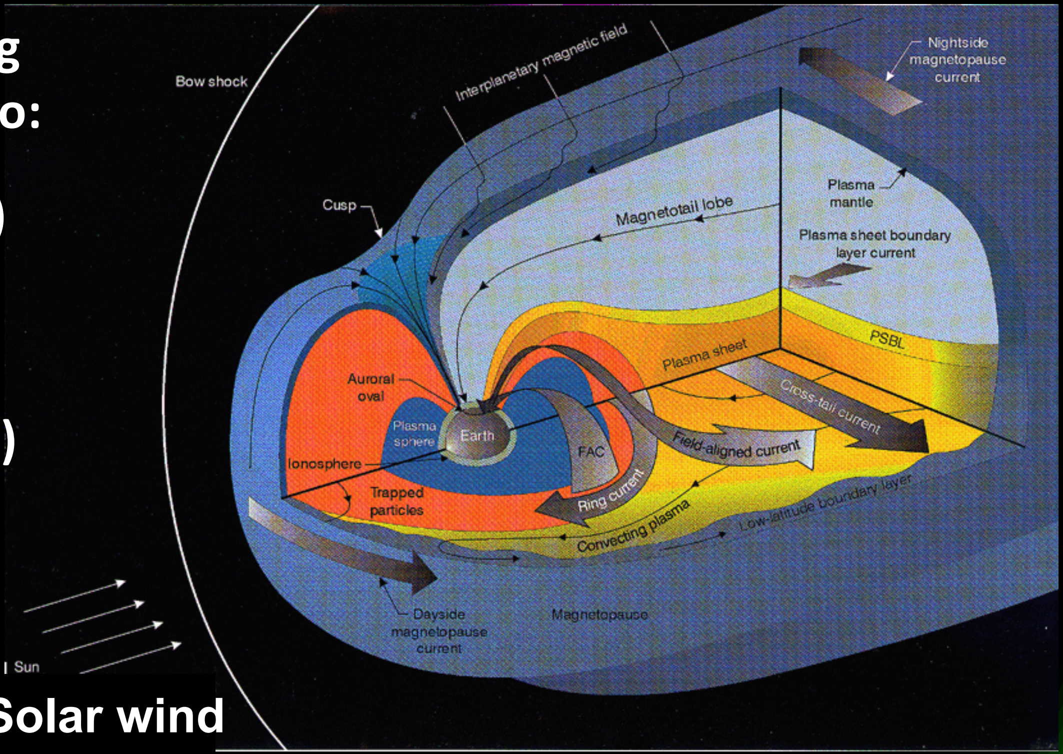

Solar wind

=> Quantitative estimates are needed!

EM energy transfer and Joule heating

- In the steady state, the energy flow between the ionospheric plasma volume and the Poynting's flux

$$\nabla \cdot \mathbf{S} + \mathbf{j} \cdot \mathbf{E} = 0$$

S - Poynting's vector
j - Ionospheric current density
E - Electric field

- Energy exchange rates in the ionosphere

$$\mathbf{j} \cdot \mathbf{E} = \mathbf{j} \cdot (\mathbf{E} + \mathbf{u} \times \mathbf{B}) + \mathbf{u} \cdot (\mathbf{j} \times \mathbf{B})$$

B - Magnetic field
u – neutral wind

q_{EM}: Electromagnetic energy exchange rate

q_J: Joule heating (ion-neutral frictional heating) rate

q_m: Mechanical energy transfer rate to/from neutral wind

EISCAT CP2 experiment

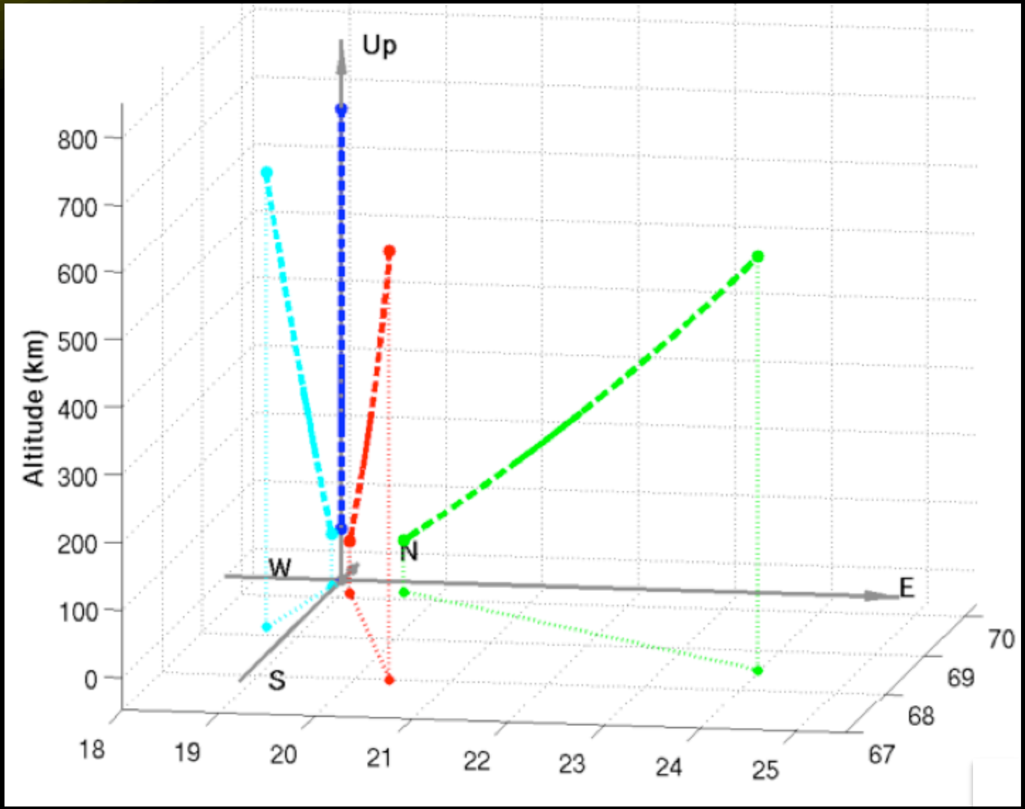

- 4 (or 3) -position scan is used to get ion velocity vectors at different altitudes.
- Both the electric field and the E-region neutral winds are estimated by utilizing a method based on stochastic inversion (Nygrén et al., JGR 2011).

Tromso: Statistical electric fields

Aikio, Cai and Nygrén, JGR 2012

- **With increasing Kp, E_N increases and maximum is observed at earlier MLT (related to the expansion of the auroral oval)**
- **EF is dominated by the north-south component, east-west component is small**

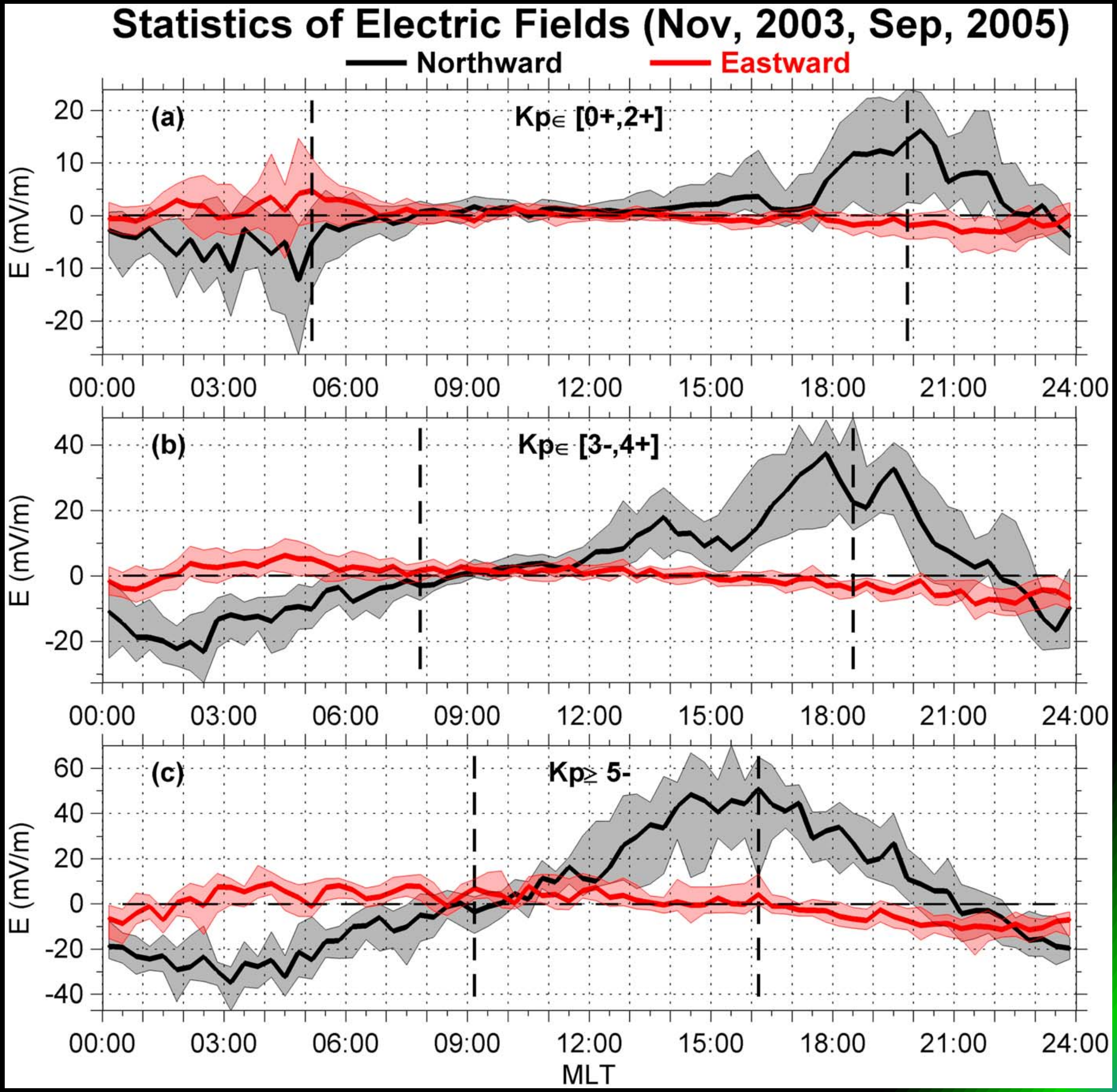

Example day, TRO 19 Sep 2005

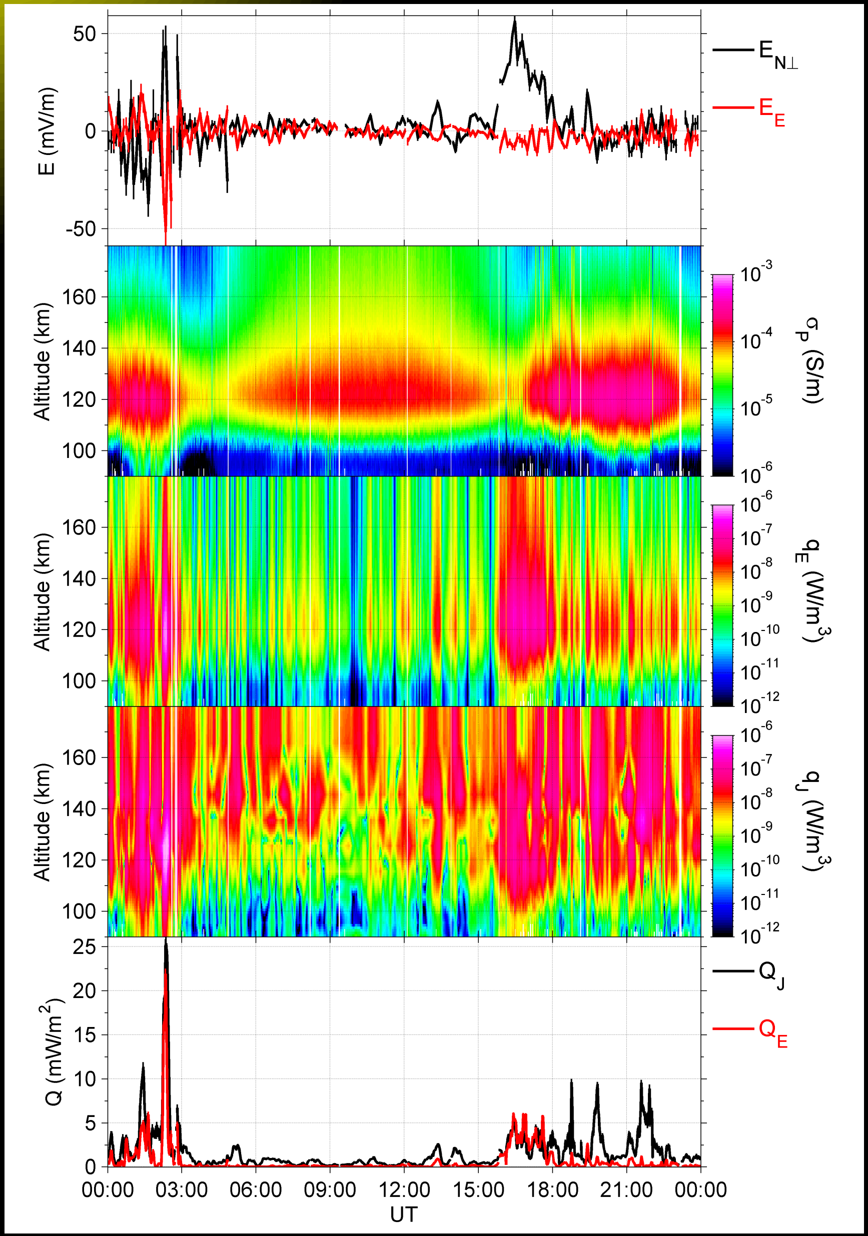

Two electric field E components

Electrical Pedersen conductivity $\sigma_P(z)$

Generally used proxy for Joule heating
$q_E(z) = \sigma_P(z)\, E^2$

Joule heating with E-region neutral winds
$q_J(z) = \sigma_P(z)\, |\mathbf{E} + \mathbf{u}(z) \times \mathbf{B}|^2$

Height-integrated (70 – 180 km) Joule heating rates $Q_J = \quad q_J(z)$

ESR (75º MLAT) Joule heating hot spot

- All CP-2 measurements 2002-2015 by ESR (230 days) were analyzed and the afternoon hot spot was still visible in statistical results.
- Appears during all seasons, but values obey: summer>equinox>winter indicating that background conductance plays a role.
- Appears both for northward and southward IMF conditions, but values are stronger during southward IMF conditions.

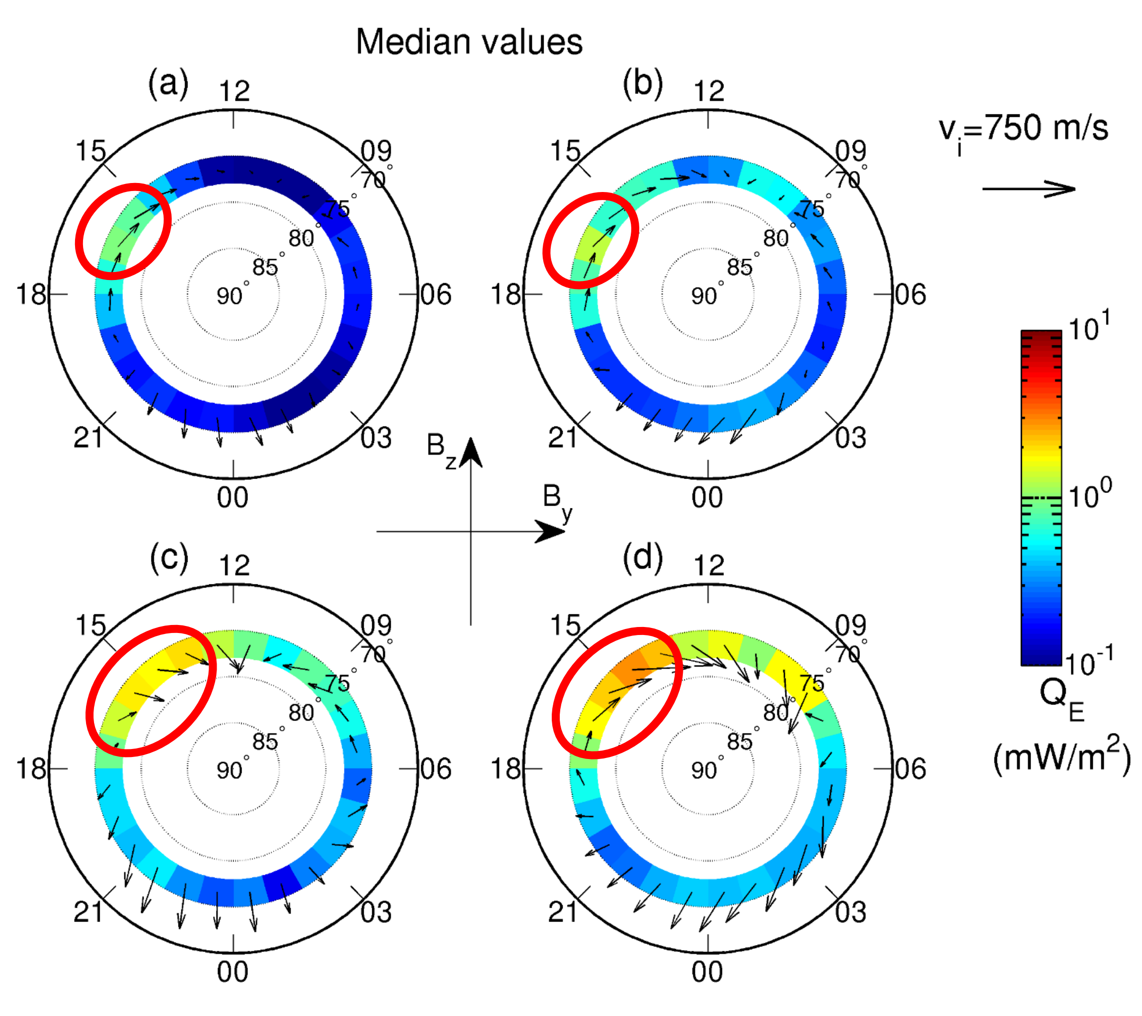

Equinox

Cai, Aikio and Milan, in press, JGR 2016

Occurs during dayside magnetic reconnection

- During slow-speed solar wind, the dominant IMF direction is southward, which is the general requirement for the low-latitude magnetic merging at the dayside magnetopause.
- During high-speed solar wind, the IMF may point also in the northward direction, provided that the IMF |By| is large, which makes the dayside magnetopause merging also possible.

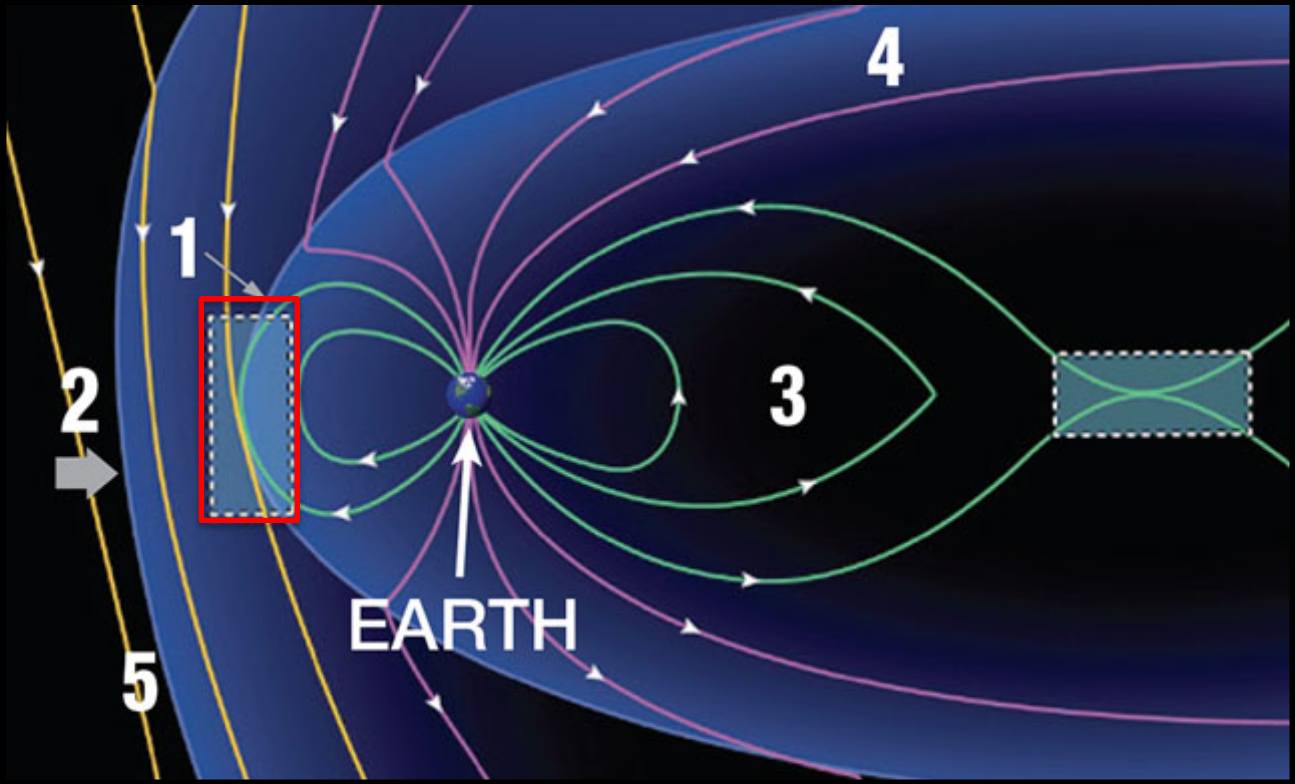

Joule heating hot spot – auroral hot spot?

- Only a couple of optical images have been found for ESR hot spot events so far, an example is shown below.

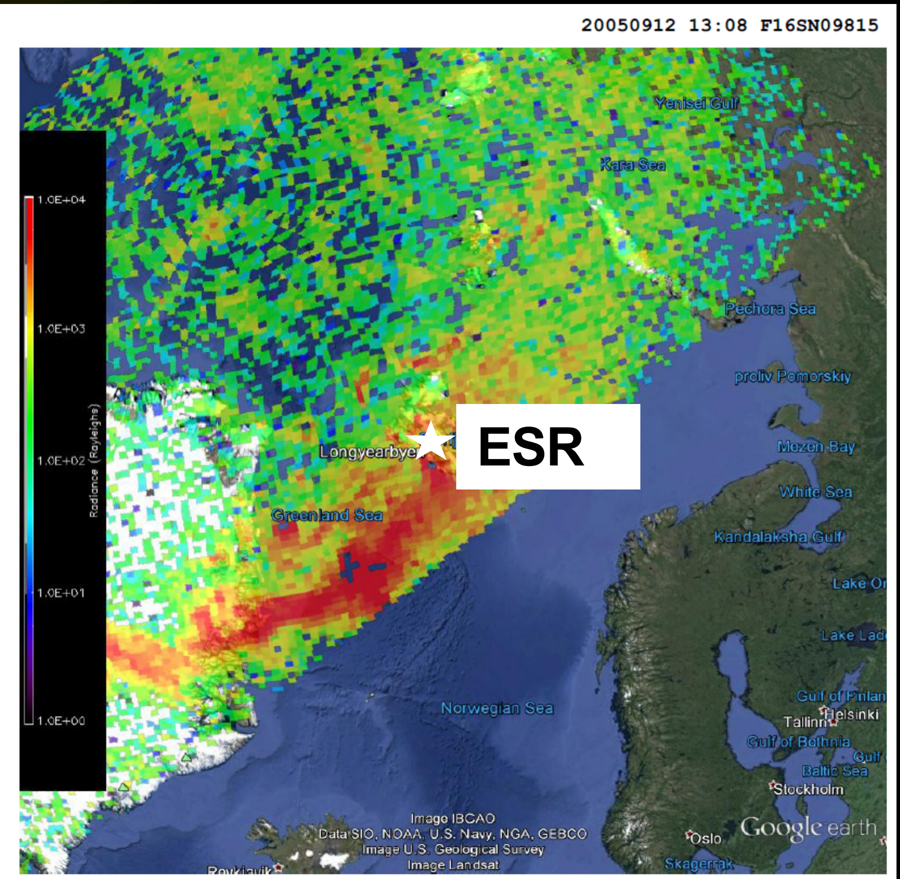

LBH intensity measured by DMSP/F16 SSUSI on 12 Sep 2005

- **Is there a relationship between the afternoon Joule heating hot spot and the auroral hot spot at about the same location found in optical images by Cogger et al. (1977) and Murphree et al. (1981)?**
- **We need multi-instrument observations around the hot spot.**
- **Global modeling for selected events may help us to understand the physics of event drivers.**